

DENSITY FLUCTUATIONS IN THE SOLAR WIND DRIVEN BY ALFVÉN WAVE PARAMETRIC DECAY

TREVOR A. BOWEN,¹ SAMUEL BADMAN,¹ PETR HELLINGER,² AND STUART D. BALE¹

¹*Physics Department and Space Sciences Laboratory, University of California, 7 Gauss Way, Berkeley, CA 94720, USA*

²*Astronomical Institute, CAS, Bocni II/1401, CZ-14100 Prague, Czech Republic*

Submitted to ApJL

ABSTRACT

Measurements and simulations of inertial compressive turbulence in the solar wind are characterized by anti-correlated magnetic fluctuations parallel to the mean field and density structures. This signature has been interpreted as observational evidence for non-propagating pressure balanced structures (PBS), kinetic ion acoustic waves, as well as the MHD slow-mode. Given the high damping rates of parallel propagating compressive fluctuations, their ubiquity in satellite observations is surprising, and suggestive of a local driving process. One possible candidate for the generation of compressive fluctuations in the solar wind is Alfvén wave parametric instability. Here we test the parametric decay process as a source of compressive waves in the solar wind by comparing the collisionless damping rates of compressive fluctuations with the growth rates of the parametric decay instability daughter waves. Our results suggest that generation of compressive waves through parametric decay is overdamped at 1 AU, but that the presence of slow-mode like density fluctuations is correlated with the parametric decay of Alfvén waves.

Keywords: instabilities — plasmas — solar wind

arXiv:1712.09336v1 [physics.space-ph] 23 Dec 2017

1. INTRODUCTION

Observations of the solar wind contain a characteristic anti-correlation between density fluctuations and magnetic perturbations parallel to the mean magnetic field. [Tu & Marsch \(1994\)](#) interpreted observed correlations on hourly timescales between magnetic pressure, thermal pressure, and density fluctuations from *Helios* as non-propagating pressure balance structures (PBS). Using spacecraft potential measurements as a proxy for density fluctuations, [Kellogg & Horbury \(2005\)](#) reported the presence of this anti-correlation in *Cluster* data, noting that PBS are consistent with the perpendicular limit of the ion-acoustic wave. [Yao et al. \(2011\)](#), using a wavelet coherence analysis, demonstrated this anti-correlation through the range of inertial scales; subsequent work interpreted these observations as PBS driven by either slow-mode or mirror modes arising from temperature anisotropies ([Yao et al. 2013a,b](#)). Through statistical analysis of a decade of *Wind* observations, [Howes et al. \(2012\)](#) attributed the compressible component of magnetic fluctuations entirely to the kinetic slow-mode. However, comparisons between a decade of *Wind* observations and numerical predictions made in both kinetic and MHD simulations by [Verscharen et al. \(2017\)](#) suggest that the MHD slow-mode best explains the compressible component of the solar wind.

Strong collisionless Landau damping of kinetic slow-mode waves propagating parallel to the magnetic field is expected for solar wind parameters at 1 AU ([Barnes 1966](#)). For this reason the generation, presence, and damping of kinetic slow-mode fluctuations in the solar wind remains an open question in space physics. [Klein et al. \(2012\)](#) argued that the distribution of slow-mode waves in the solar wind is consistent with critically balanced turbulence, in which non-linear interactions between Alfvénic and slow-mode fluctuations cascade weakly damped perpendicular compressible fluctuations at large scales to smaller parallel scales. The damping of these waves could provide a source of heating in the solar wind ([Narita & Marsch 2015](#)).

In this letter, we explore the parametric decay instability (PDI) as a process for generating compressive fluctuations in the solar wind. In MHD, the PDI decay process is recognized as the instability of circularly polarized Alfvén eigenmodes at high fluctuation amplitudes ([Derby 1978](#); [Goldstein 1978](#)). For low β plasmas, the large amplitude Alfvénic fluctuation (mother wave) couples to two daughter waves: a parallel propagating compressive fluctuation, and a backwards propagating Alfvén wave. A class of parametric instabilities exist outside the low β PDI decay: e.g. at $\beta \gtrsim 1$ the instability is dominated by the growth of forward propagating

Alfvénic daughter waves at twice the mother wave frequency ([Jayanti & Hollweg 1993](#); [Hollweg 1994](#)).

For the low β decay instability, simulations of high amplitude circularly polarized Alfvén waves have verified the process in the MHD regime, and have suggested that PDI daughter waves can seed turbulent cascades [Del Zanna et al. \(2001\)](#); [Tenerani & Velli \(2013\)](#); [Malara et al. \(2001\)](#). Simulations have extended the PDI to large amplitude Alfvén waves with arc and linear polarizations, non-monochromatic distributions of waves, as well as to oblique propagation [Del Zanna \(2001\)](#); [Matteini et al. \(2010\)](#); [Del Zanna et al. \(2015\)](#). Furthermore, kinetic simulations have recovered parametric instabilities in multi-species models, albeit with decrease in growth rate relative to the fluid regime, and have demonstrated the preferential heating of α particles as well as proton core heating and beam formation [Araneda et al. \(2008\)](#); [Araneda et al. \(2009\)](#); [Kauffmann & Araneda \(2008\)](#). Numerical simulations of PDI in a turbulent solar wind have shown the generation of slow-mode fluctuations from the decay of Alfvénic fluctuations in a relatively robust theoretical scenario [Shi et al. \(2017\)](#).

2. DATA

We use 10 years of solar wind measurements at 1AU from the NASA *Wind* mission ranging from 1996 January 1 through 2005 December 31. Data from the Magnetic Field Investigation (MFI) [Lepping et al. \(1995\)](#), Solar Wind Experiment (SWE) [Ogilvie et al. \(1995\)](#), and Three Dimensional Plasma (3DP) experiment [Lin et al. \(1995\)](#) are separated into non-overlapping 300 second intervals. Individual intervals are excluded when *Wind's* geocentric distance is less than $35R_E$, the average magnitude of solar wind speed is < 250 km/s, or if an interval is missing $> 15\%$ of coverage from any instrument. Data gaps are interpolated when $< 15\%$ of measurements are missing. Additionally, intervals are excluded if there is significant discrepancy between 3DP and SWE measurements of mean proton density such that $(n_{SWE} - n_{3DP})/n_{SWE} > 0.1$. The resulting data set consists of 533222 intervals of 300 seconds. Techniques from [Pulupa et al. \(2014\)](#) were used to obtain electron densities and temperatures for 282286 of these intervals.

The 3 s cadence 3DP "on board" proton moment measurements are interpolated to the MFI time base. Measurements of n , \mathbf{v} , and \mathbf{B} are then separated in to mean and fluctuation quantities in the form of $\mathbf{B} = \mathbf{B}_0 + \delta\mathbf{B}$. Mean quantities are determined through time averaging each 300 s interval, denoted as $\langle \dots \rangle$. Vector fluctuations are rotated into a field aligned coordinate (FAC) sys-

tem, $\delta\mathbf{B}_{FAC} = (\delta B_{\perp 1}, \delta B_{\perp 2}, \delta B_{\parallel})$, defined with $\hat{\mathbf{e}}_3 = \mathbf{B}_0/|B_0|$. For each interval, scalar fluctuations are characterized through root-mean-square (RMS) quantities normalized to the mean interval value

$$\bar{\delta n} = \sqrt{\langle \delta n^2 \rangle} / n_0.$$

Vector fluctuations are separated into parallel and perpendicular RMS values of the form

$$\delta\bar{B}_{\perp} = \frac{\sqrt{\langle \delta B_{\perp}^2 \rangle}}{B_0} = \frac{\sqrt{\langle \delta B_{\perp 1}^2 + \delta B_{\perp 2}^2 \rangle}}{B_0}$$

and

$$\delta\bar{B}_{\parallel} = \frac{\sqrt{\langle \delta B_{\parallel}^2 \rangle}}{B_0}.$$

The FAC fluctuation quantities are used in deriving Elsässer variables,

$$\mathbf{z}^{\pm} = \delta\mathbf{v}_{FAC} \pm \delta\mathbf{b}_{FAC};$$

normalized cross helicity,

$$H_c = \frac{\langle \delta\mathbf{b}_{FAC} \cdot \delta\mathbf{v}_{FAC} \rangle}{\langle \delta b^2 \rangle + \langle \delta v^2 \rangle};$$

and the zero lag cross correlation between parallel field fluctuations and density,

$$C(\delta n, \delta B_{\parallel}) = \frac{\sum_{i=0}^{N-1} \delta n_i \delta B_{\parallel i}}{\sqrt{\sum_{i=0}^{N-1} \delta n_i^2} \sqrt{\sum_{i=0}^{N-1} \delta B_{\parallel i}^2}}.$$

Where the magnetic field has been normalized to dimensions of velocity using $\delta\mathbf{b} = \delta\mathbf{B}/\sqrt{\mu_0 n_p m_p}$.

3. CALCULATION OF PROPAGATION DIRECTION

Calculating the propagation directions for shear MHD Alfvén waves is typically implemented with a minimum variance analysis (Yao et al. 2013a). The minimum variance direction is acquired through diagonalizing the covariance matrix of $\delta\mathbf{B}$. As the shear Alfvén wave consists of only transverse fluctuations, the minimum eigenvalue direction yields an estimate of the shear Alfvén propagation direction.

For the slow-mode wave with propagation vector confined to the $\hat{\mathbf{e}}_1$ - $\hat{\mathbf{e}}_3$ plane it can be shown that $\delta\mathbf{v} = (\delta v_{\perp}, 0, \delta v_{\parallel})$ and $\mathbf{k} = (k_{\perp}, 0, k_{\parallel})$. Because of the longitudinal fluctuations associated with the slow-mode wave, the minimum variance analysis does not resolve the propagation direction. However, from the linearized MHD induction equation $\omega\delta\mathbf{B} = (\mathbf{k} \cdot \mathbf{v})\mathbf{B}_0 - (\mathbf{k} \cdot B_0)\delta\mathbf{v}$, it is readily derived that

$$\frac{\omega\delta\mathbf{B}}{v_x B_0} = k_x \hat{z} - k_z \hat{x},$$

leading to

$$\tan\theta_{sm} = \frac{k_{\perp}}{k_{\parallel}} = \frac{\delta B_{\parallel}}{\delta B_{\perp}},$$

where θ_{sm} gives the propagation angle of the slow-mode wave relative to the mean magnetic field. The slow-mode propagation angle agrees with the minimum variance prediction for a shear Alfvén wave in the limit of $\delta B_{\parallel} = 0$.

Figure 1 (top) shows the joint probability distributions of H_c and θ_{sm} . The distribution is column-normalized to the most probable cross helicity at each angle. A decrease in cross helicity is observed with increasing propagation angle, capturing the decrease in Alfvénicity with increase in compressive fluctuations. Figure 1 (bottom) shows the the column normalized joint distribution of $C(\delta n, \delta B_{\parallel})$ and θ_{sm} . The transition to highly anti-correlated density δn and parallel magnetic fluctuations δB_{\parallel} occurs at approximately the same propagation angle, $\theta_{sm} \sim 25^\circ$, as the decrease in cross helicity. Two regimes are apparent: quasi-parallel Alfvénic like intervals with large cross helicity, and highly compressible intervals with mixed cross helicity and strong density-field correlations consistent with slow-mode fluctuations. The distribution of data between Alfvénic and slow-mode fluctuations is consistent with the results of Klein et al. (2012). Howes et al. (2012) restricted analysis to intervals with $\delta n > 0.5 \text{ cm}^{-3}$, arguing that lower density intervals may be subject to instrumental noise; the uniform and simultaneous transition from Alfvénic to slow-mode-like qualities in both H_c and $C(\delta n, \delta B_{\parallel})$ without such a restriction suggests that our analysis is largely insensitive to noise in the density data at low amplitudes.

4. DAMPING

Historically, presence of kinetic slow-mode fluctuations in the solar wind has been questioned due to the heavy collisionless damping expected in solar wind plasma at 1 AU. (Barnes 1966). The transition of Alfvénic to slow-mode-like fluctuations depicted in Figure 1 reveals the presence of compressive fluctuations with relatively parallel propagation (e.g. $\theta_{sm} \sim 25^\circ$). In contrast, Verscharen et al. (2017) argue that observations of the compressive solar wind plasma are best represented as oblique, weakly damped, MHD slow-mode waves which may propagate more freely through the heliosphere. Gary (1993) gives the ion acoustic (IA) damping rate for a thermal plasma with Maxwellian distribution as

$$\gamma \simeq -|k_{\parallel}|c_s\sqrt{\pi}\frac{c_s^3}{w_{\parallel p}^3}\frac{e^{-c_s^2/w_{\parallel p}^2}}{1+3w_{\parallel p}^2/c_s^2} \quad (1)$$

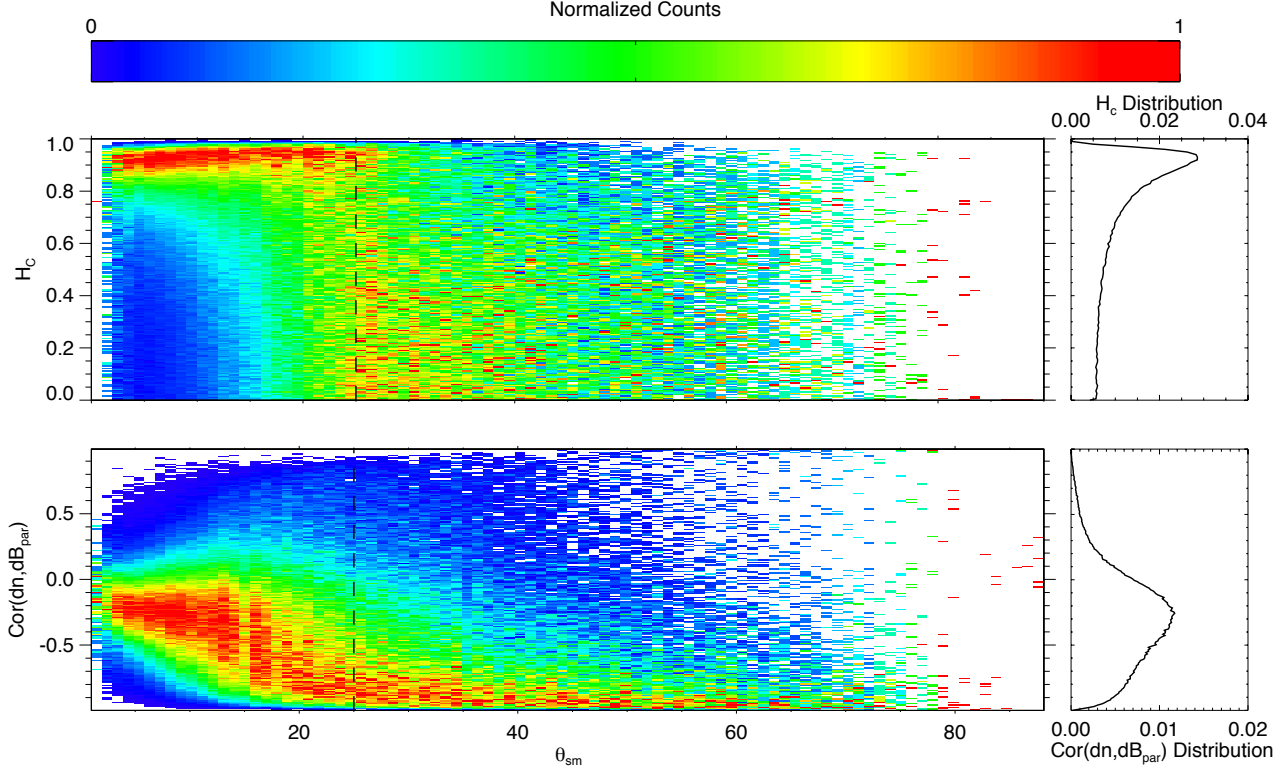


Figure 1. (Top) Joint distribution of measurements of normalized cross helicity, H_c and slow-mode propagation angle θ_{sm} . The data is column normalized within each angle bin (1° resolution). The 1-d distribution of H_c observations is plotted to the right. (Bottom) Joint distribution of the density-parallel magnetic fluctuation cross-correlation, $C(\delta n, \delta B_{\parallel})$, and the slow-mode propagation angle, θ_{sm} . The data are again column normalized within each angle bin with the 1-d distribution of $C(\delta n, \delta B_{\parallel})$ observations plotted to the right. A dashed line identifies the transition between Alfvénic and slow-mode fluctuations at $\theta_{sm} \sim 25^\circ$.

where $k_{\parallel} = k \cos \theta_{sm}$, $w_{\parallel p} = \sqrt{2k_B T_{\parallel p}}$, and the sound speed is

$$c_s = \sqrt{\frac{3k_b T_{\parallel p} + ek_b T_{\parallel e}}{m_p}}.$$

Figure 2 shows IA damping rates computed for each interval normalized to the solar wind expansion time $t_{exp} = 1\text{AU}/V_{sw}$ as a function of θ_{sm} . Data are restricted to intervals where fits of electron distributions were available (Pulupa et al. 2014). The majority of expansion time normalized damping ages are above 10, and uniformly above unity, suggesting that even moderate to highly oblique propagating kinetic slow-mode like fluctuations should undergo significant damping over 1 AU propagation.

Figure 3 (top) shows the column normalized joint distribution of δn and $C(\delta n, \delta B_{\parallel})$. It is evident that the slow-mode correlation emerges as the density fluctuations increase in amplitude. Figure 3 (bottom) shows that this correlation emerges even when data is restricted to quasi-parallel propagation directions with $\theta_{sm} < 20^\circ$. If these fluctuations are associated with a strongly damped

kinetic slow-mode, then their presence at 1 AU demands the presence of a local driving source.

5. PARAMETRIC DECAY

To test whether parametric coupling between wave modes generate compressive fluctuations from the decay of large amplitude Alfvénic fluctuations we compare our observations with analytically derivable parametric growth rates. Following Derby (1978) and Goldstein (1978), a dispersion relation for the evolution of a compressive wave coupled to an MHD mother wave is given by:

$$(\omega + k + 2)(\omega + k - 2)(\omega - k)(\omega^2 - \beta k^2) - \left(\frac{\delta B_{\perp}}{B_0}\right)^2 k^2 (\omega^3 + k\omega^2 - 3\omega + k) = 0. \quad (2)$$

This 5th order polynomial, with k and ω corresponding to wave number and frequency of the compressive daughter wave in units of the mother wave, depends only on β and $\delta B_{\perp}/B_0$. There is a small range of

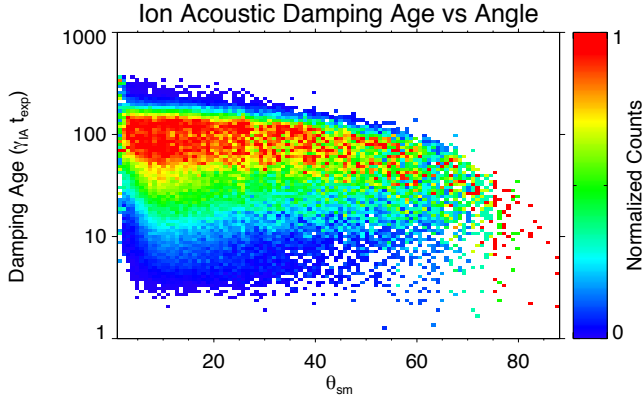


Figure 2. Joint distribution of the expansion normalized ion-acoustic damping rates, $\gamma_{IA} t_{exp}$, ($t_{exp} = 1\text{AU}/V_{sw}$) and slow-mode propagation angle θ_{sm} . Data is restricted to intervals with fitted electron temperatures. The distribution is column normalized in each angle bin (1° resolution). Damping ages, $\gamma_{IA} t_{exp}$, are uniformly much greater than unity, suggesting strong damping of ion acoustic fluctuations even at oblique and quasi-perpendicular propagation angles. At low propagation angles $\gamma_{IA} t_{exp} \sim 100$ while at quasi-perpendicular angles typically $\gamma_{IA} t_{exp} \gtrsim 10$.

$k_L < k < k_U$ for which a single conjugate pair of complex solutions $\omega = \omega_0 \pm i\gamma_{pd}$ exist. The parametric growth rate γ_{pd} , corresponding to the fastest growing decay product, is determined numerically given observed values of β and $\delta\bar{B}_\perp$.

Figure 4 (left) shows the joint distribution of our observations of $\delta\bar{B}_\perp$ and β . Contours of the numerically determined γ_{pd}/ω_0 , plotted as solid black lines, bound the data at about 0.05-0.1, suggesting that the solar wind at 1 AU is bounded by high PDI growth rates. Figure 4 (right) shows the same distribution of $\delta\bar{B}_\perp$ and β with the average value of $\delta\bar{n}$ projected onto the plane. The median $\delta\bar{n}$ is 0.034, with a range of [0.01, 1.10]. Our results show that intervals with the largest density fluctuations correspond to intervals of high parametric growth rates.

Two sets of contours are overlaid in Figure 4 (right). The first set, $\gamma_{pd} t_{exp}$ plotted in red, correspond to PDI growth rates normalized to the solar wind expansion time $t_{exp} = 1\text{AU}/v_{sw}$. In order to normalize γ_{pd} to the expansion timescale, estimates for parametric instability growth rates γ_{pd} with physical units of s^{-1} are constructed using the numerically calculated γ_{pd}/ω_0 , where

$$\omega_0 = \text{median}(V_{alf}) \cdot \text{median}(k_{\parallel}).$$

Here k is given by the Taylor hypotheses, $k = 1/(\tau v_{sw})$, where τ is the length of each interval (300 s), $k_{\parallel} = k \cos\theta$, and we assume a highly oblique propagation of $\theta = 80^\circ$. Additionally, we consider only median values of intervals with $\beta < 0.5$ where PDI growth is most relevant

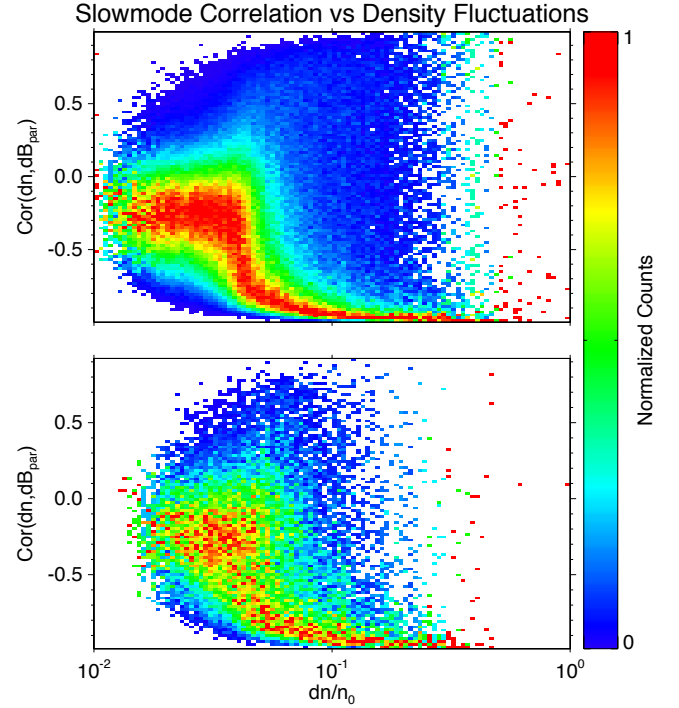


Figure 3. (Top) Joint probability distribution of density-parallel magnetic fluctuation cross-correlation, $C(\delta n, \delta B_{\parallel})$, and density fluctuation amplitude, $\delta\bar{n}$. (Bottom) Restricting data to intervals with $\beta < 0.5$ with $\theta_{sm} < 20^\circ$ reveals the presence of fluctuations with slow-mode like density-field correlations propagating parallel to the mean magnetic field. Data are column normalized to the most probable value of $C(\delta n, \delta B_{\parallel})$ for each $\delta\bar{n}$ bin.

and the MHD slow-mode is approximated by IA fluctuations. The median values for V_{sw} and V_{alf} are 410 km s^{-1} and 95 km s^{-1} with standard deviations of 95 km s^{-1} and 67 km s^{-1} respectively. These values correspond to a typical fractional dispersion of 70%, roughly implying that the distribution of observations is bounded by $\sim 3 - 10$ growths of the parametric decay. Though the growth rate of the parametric decay is relatively small at 1AU, the propagation of these intervals through the heliosphere allows for several growths of the parametric decay. Additionally, Figure 4 (right) shows that intervals which undergo a single iteration of parametric decay demonstrate enhanced density fluctuations: suggesting that density fluctuations are correlated with the growth of compressive PDI daughter waves.

Given the strong damping of the compressive modes, it is of significant importance whether PDI produces density fluctuations faster than their dissipation. The second set of contours in Figure 4 (right) show the value $\zeta = \frac{\gamma_{pd}/\omega_0}{\gamma_{IA}/\omega_c}$ which represent size of slow-mode growth through PDI relative to their decay through collisionless

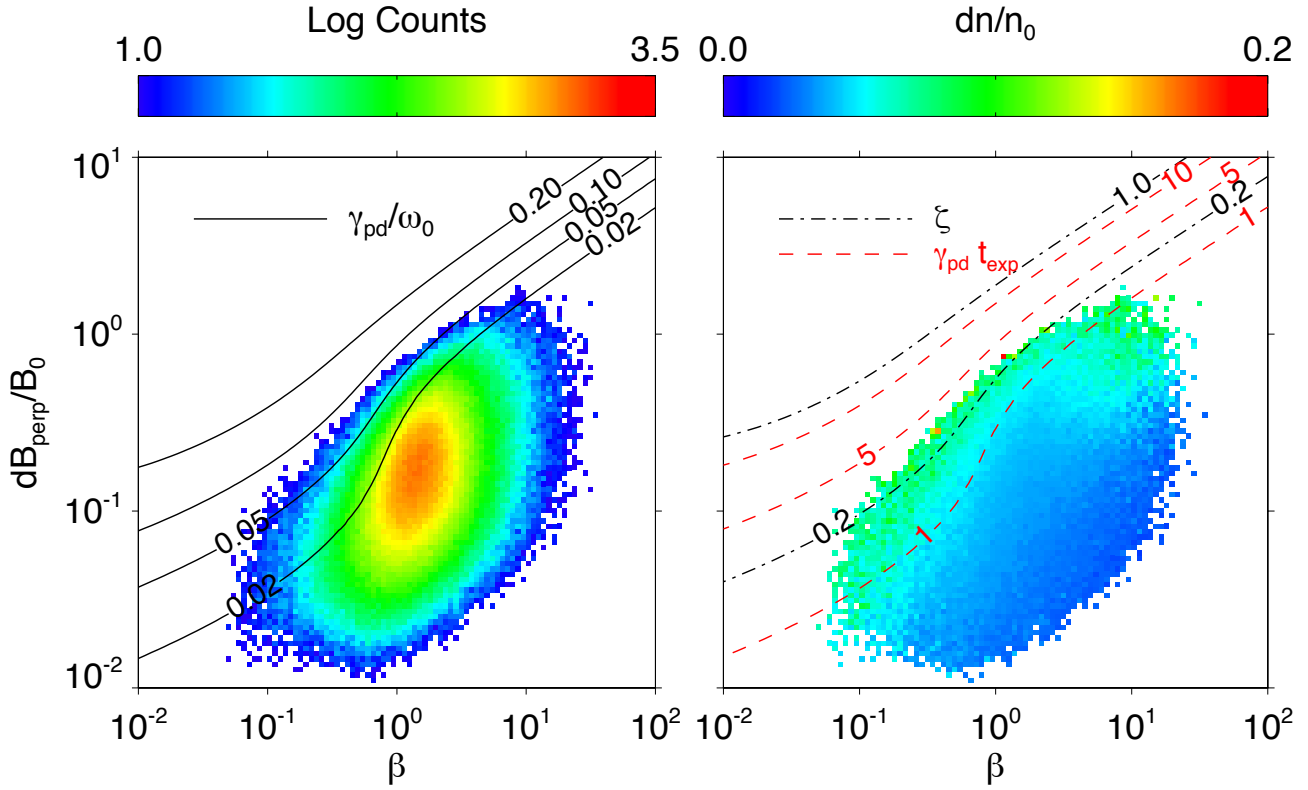


Figure 4. (Left) Joint 2-d distribution of $\delta\bar{B}_\perp$ and β . Contours of the parametric growth rate normalized to the linear wave frequency are shown as a solid black line. Data are bounded by high parametric instability growth rates. (Right) Joint 2-d distribution of $\delta\bar{B}_\perp$ and β with color scale given by mean values of δn . Contours of the expansion normalized parametric decay rate, $\gamma_{pd} t_{exp}$, are shown in dashed red lines. Though PDI growth rates are quite small, several iterations of the decay may occur over 1 AU propagation. Contours of the ratio between PDI growth and IA damping are given ζ are shown in dashed black lines. Though the highest amplitude density fluctuations correspond to the largest values of ζ , the generation of density fluctuations through PDI is overdamped.

damping. Using ζ , rather than e.g. γ_{pd}/γ_{IA} , removes dependence of propagation direction of both mother and daughter waves. High values of ζ presumably indicate the presence of driven compressive daughter waves. Intervals with low values of ζ should dissipate compressive fluctuations faster than the PDI can drive them. Figure(4) shows that though intervals with large density fluctuations occur with greater values of ζ , compressive fluctuations driven by parametric decay are overdamped by the IA rate.

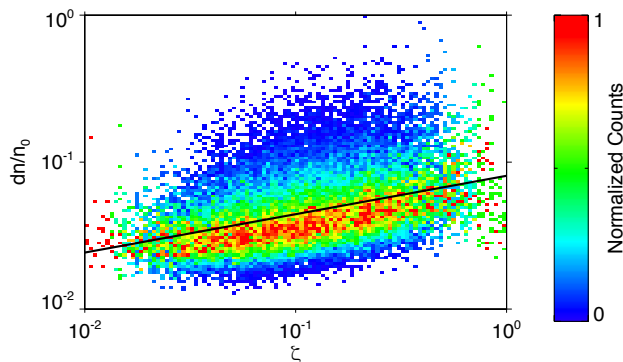


Figure 5. 2-d distribution of $\bar{\delta n}$ and ζ . Data is column normalized to each ζ bin. A least squares fit to the data, shown as a black line, gives a power law slope of 0.25 and a Pearson correlation of 0.36.

Figure 5 shows the scaling of $\bar{\delta n}$ with ζ . Data are again restricted to $\beta < 0.5$ intervals, where the parametric instability is known to generate compressive daughter waves. A positive correlation is observed between the density fluctuations and ζ . A least squares fit in logarithmic space suggests a power law relationship of $\bar{\delta n} \sim (\zeta)^{0.26}$ with a Pearson cross correlation of $\rho = 0.36$; however we note that approximately 99% of the data are over-damped. When a least square fit is performed between $\bar{\delta n}$ and the dimensionless parametric growth rate, γ_{pd}/ω_0 we recover a powerlaw relation of $\bar{\delta n} \sim (\gamma_{pd}/\omega_0)^{0.26}$ and a Pearson correlation of $\rho = 0.37$. Suggesting that the density fluctuations $\bar{\delta n}$ are weakly dependent on the IA damping rate. Additionally, the positive correlation between parametric instability growth rate and density fluctuations in the solar wind suggests that compressive fluctuations may be related to daughter waves of the parametric decay process. Both of these correlations are stronger than the correlation between just the amplitudes of $\delta \bar{B}_\perp$ and $\bar{\delta n}$, for which we find $\rho = 0.24$.

6. DISCUSSION

Our results show that the compressive component of solar wind plasma is not restricted to weakly damped fluctuations propagating perpendicular to the magnetic field. If these compressive fluctuations are related to a kinetic slow-mode, their presence likely requires an active driving process. Previous work has invoked a scalar turbulent cascade to explain the replenishing of slow-mode like fluctuations (Klein et al. 2012; Chen et al. 2012). In this letter we suggest that the parametric coupling of large amplitude Alfvén waves to compressional modes may drive slow-mode like fluctuations in the solar wind. We consider parametric decay as a parallel process; however, the decay of an oblique shear Alfvén wave generates a spectrum of fluctuations over a range of angles with respect to the ambient magnetic field (Matteini et al. 2010). Additionally, though the parametric growth rate used in this paper is relevant for low β plasmas, recent work has suggested that pressure anisotropies may extend the range of β for which parametric growth is possible (Derby 1978; Tenerani et al. 2017).

The existence of parametric coupling has been verified in both analytic and computational studies but has yet to be observed in the solar wind. The parametric instability is an attractive physical mechanism as it can explain the seeding of backwards Alfvénic fluctuations required for non-linear interactions leading to a critically balanced turbulent cascade in the solar wind (Tenerani & Velli 2013; Malara et al. 2001). Additionally, parametric coupling preferentially excites slow-mode rather than fast-mode compressions; this may provide additional explanation to observed distribution of fluctuations observed at 1 AU: Alfvénic $\sim 90\%$, slow-mode $\sim 10\%$, and very little fast-mode contribution (Klein et al. 2012).

Our observations from *Wind* show that the distribution of data is bounded by high parametric growth rates. This suggests that parametric processes may limit the amplitude of Alfvénic fluctuations. Furthermore, our results show that the marginally stable intervals of solar wind have likely undergone several (1-10) growths of the parametric decay over their propagation to 1AU. These intervals additionally demonstrate enhanced density fluctuations consistent with slow-mode daughter-waves.

In low β observations, we find that density fluctuations are well correlated with the parametric growth rate, suggesting that compressive fluctuations could be daughter waves of the parametric instability. However we must note that the growth of compressive fluctuations through PDI appears overdamped by the IA damping rate given in Equation 1. In light of this, we high-

light the results of [Verscharen et al. \(2017\)](#), which suggest that the compressive slow-mode may have lower damping rates. Reducing IA damping rates by approximately a factor of 5 would provide underdamped growth of compressive fluctuations through PDI.

Previous studies, e.g. [Tenerani & Velli \(2013\)](#), have demonstrated an increase in PDI growth rates closer in the heliosphere using WKB propagation in an expanding fluid. Such scaling suggesting that compressive waves are more easily generated through PDI near the sun. The launch of the NASA Parker Solar Probe mission in July 2018 will likely reveal whether parametric coupling between fluctuations play an increased role in the inner heliosphere.

In considering the growth rate of the PDI relative to the linear wave time, ω_0 we do not take into account the effect of turbulence solar wind. It is likely that the non-linear interaction time between Alfvénic fluctuations may play an important role. Specifically, it is likely that a critically balanced cascade where non-linear interactions occur on order the wave propagation time

could hamper parametric coupling between Alfvénic and slow-mode like fluctuations [Schekochihin et al. \(2009\)](#). This idea has been touched upon in [Shi et al. \(2017\)](#), in which PDI growth rates were found to be reduced in a turbulent plasma. Our future work looks to address the physics of parametric coupling in a turbulent plasma and to compare the growth of compressive modes through PDI versus their recycling through a turbulent cascade.

The authors would like to acknowledge helpful discussions with Marco Velli, Anna Tenerani, and Alfred Mallet. We would additionally like to extend our thanks to Marc Pulupa and Chadi Salem for providing processed electron data from Wind/3DP. T.A.B. is supported by NASA Earth and Space Science Fellowship NNX16AT22H. P.H. acknowledges grant 18-08861S of the Czech Science Foundation. Wind/3DP data analysis at UC Berkeley is supported in part by NASA grant NNX16AP95G.

REFERENCES

- Araneda, J. A., Maneva, Y., & Marsch, E. 2009, *Physical Review Letters*, 102, 175001
- Araneda, J. A., Marsch, E., & F.-Viñas, A. 2008, *Phys. Rev. Lett.*, 100, 125003
- Barnes, A. 1966, *Physics of Fluids*, 9, 1483
- Chen, C. H. K., Mallet, A., Schekochihin, A. A., et al. 2012, *ApJ*, 758, 120
- Del Zanna, L. 2001, *Geophys. Res. Lett.*, 28, 2585
- Del Zanna, L., Matteini, L., Landi, S., Verdini, A., & Velli, M. 2015, *Journal of Plasma Physics*, 81, 325810102
- Del Zanna, L., Velli, M., & Londrillo, P. 2001, *A&A*, 367, 705
- Derby, Jr., N. F. 1978, *ApJ*, 224, 1013
- Gary, S. P. 1993, *Theory of Space Plasma Microinstabilities*, 193
- Goldstein, M. L. 1978, *ApJ*, 219, 700
- Hollweg, J. V. 1994, *J. Geophys. Res.*, 99, 23
- Howes, G. G., Bale, S. D., Klein, K. G., et al. 2012, *ApJL*, 753, L19
- Jayanti, V., & Hollweg, J. V. 1993, *J. Geophys. Res.*, 98, 19
- Kauffmann, K., & Araneda, J. A. 2008, *Physics of Plasmas*, 15, 062106
- Kellogg, P. J., & Horbury, T. S. 2005, *Annales Geophysicae*, 23, 3765
- Klein, K. G., Howes, G. G., TenBarge, J. M., et al. 2012, *ApJ*, 755, 159
- Lepping, R. P., Acuña, M. H., Burlaga, L. F., et al. 1995, *SSRv*, 71, 207
- Lin, R. P., Anderson, K. A., Ashford, S., et al. 1995, *SSRv*, 71, 125
- Malara, F., Primavera, L., & Veltri, P. 2001, *Nonlinear Processes in Geophysics*, 8, 159
- Matteini, L., Landi, S., Del Zanna, L., Velli, M., & Hellinger, P. 2010, *Geophys. Res. Lett.*, 37, L20101
- Narita, Y., & Marsch, E. 2015, *ApJ*, 805, 24
- Ogilvie, K. W., Chornay, D. J., Fritzenreiter, R. J., et al. 1995, *SSRv*, 71, 55
- Pulupa, M. P., Bale, S. D., Salem, C., & Horaites, K. 2014, *Journal of Geophysical Research: Space Physics*, 119, 647
- Schekochihin, A. A., Cowley, S. C., Dorland, W., et al. 2009, *ApJS*, 182, 310
- Shi, M., Li, H., Xiao, C., & Wang, X. 2017, *ApJ*, 842, 63
- Tenerani, A., & Velli, M. 2013, *Journal of Geophysical Research (Space Physics)*, 118, 7507
- Tenerani, A., Velli, M., & Hellinger, P. 2017, *ArXiv e-prints*, arXiv:1711.06371
- Tu, C. Y., & Marsch, E. 1994, *Journal of Geophysical Research: Space Physics*, 99, 21481
- Verscharen, D., Chen, C. H. K., & Wicks, R. T. 2017, *ApJ*, 840, 106
- Yao, S., He, J.-S., Marsch, E., et al. 2011, *ApJ*, 728, 146
- Yao, S., He, J.-S., Tu, C.-Y., Wang, L.-H., & Marsch, E. 2013a, *ApJ*, 776, 94

—, 2013b, *ApJ*, 774, 59